RESEARCH ARTICLE

Water-soluble gadolinium fullerenes Gd@C_{82}-TEGs as a potential magnetic resonance imaging contrast agent

Wanyun Liu*, **Ping Huo***, **Xiuming Zhou, Dayan Xiong**

Yichun University, Yichun, Jiangxi, China

* liuwanyun2006@163.com (WL), ycxyhuoping@163.com (PH)

Abstract

The water-soluble gadolinium fullerenes Gd@C_{82}-TEGs nanoparticles as a novel magnetic resonance imaging (MRI) contrast agent were fabricated by the metal fullerenes Gd@C_{82} assembled with tetraethylene glycol (TEG). The loading Gd amount in Gd@C_{82}-TEGs nanoparticles was 8.0 wt%. The average particle size of water-soluble Gd@C_{82}-TEGs nanoparticles was 97 nm and the nanoparticles were uniformly spherical shape and had good dispersibility and no aggregation. The 97 nm spherical shape of Gd@C_{82}-TEG nanoparticles ensured high relaxivity. The proton relaxivity (r_1) and transverse relaxivity (r_2) were high up to 37.1 $mM^{-1}{\cdot}s^{-1}$ and 64.9 $mM^{-1}{\cdot}s^{-1}$, which greater than that of commercial Magnevist under the same conditions. The Gd@C_{82}-TEGs nanoparticles exhibited pronounced T_1-weighted MRI *in vitro*. The MRI signal-enhancing efficiency of Gd@C_{82}-TEGs nanoparticles was superior to that of gadolinium diethylenetriamine pentaacetate Gd-DTPA (Magnevist). The Gd@C_{82}-TEGs nanoparticles had no significant effect on cell metabolism and structure, and the survival rate of cells was more than 80%, which indicated that the as-prepared Gd@C_{82}-TEGs nanoparticles were no cytotoxicity.

OPEN ACCESS

Citation: Liu W, Huo P, Zhou X, Xiong D (2026) Water-soluble gadolinium fullerenes Gd@C_{82}-TEGs as a potential magnetic resonance imaging contrast agent. PLoS One 21(4): e0346592. https://doi.org/10.1371/journal.pone.0346592

Editor: Raghvendra Bohara, National University of Ireland, Galway, IRELAND

Received: October 15, 2025

Accepted: March 22, 2026

Published: April 10, 2026

Data availability statement: All relevant data are within the manuscript.

Funding: the National Natural Science Foundation of China (No. 21764016).

Competing interests: NO authors have competing interests.

Introduction

Magnetic resonance imaging (MRI) is a high-resolution imaging method without injury and ionizing radiation, which plays an important role in clinical diagnosis, especially in cancer and tumor detection [1–5]. However, due to the lower sensitivity of MRI, about 40%~50% of MRI diagnosis requires the use of MRI enhancers (contrast agents) at present. These contrast agents usually are paramagnetic substances, which can influence the water quality sub-relaxation time in local tissues of the body and change the signal intensity, lead to produce an angiographic effect [6]. The MRI contrast agents used in clinic are mainly gadolinium (Gd) chelating agents with small molecular weight, for example gadolinium diethylenetriamine pentaacetate benzyl methyl amide Gd-DTPA-BMA (Omniscan) and gadolinium diethylenetriamine pentaacetate Gd-DTPA (Magnevist) [7,8]. However, these contrast agents are limited to

extracellular fluid contrast and have low relaxation efficiency and poor tissue targeting. The chelation of Gd^{3+} ions with ligands lead to the decrease of relaxation ability, and even under some specific conditions, the chelate will release Gd^{3+} to produce toxicity [9–13]. In addition, for some small tissues or even single cells, contrast agents with higher relaxation efficiency were needed. Hence, the exploration of novel contrast agents which meet with efficient, low toxicity and tissue specificity is important to make early diagnosis with pathological tissues.

Gadolinium fullerenes refer to a kind of embedded metal fullerenes with gadolinium atoms or clusters embedded in carbon cages. These fullerenes not only possess the paramagnetic properties of embedded gadolinium, but also maintain the properties of carbon cages, such as large specific surface area, stability and easy to be multi-functional and so on [14]. As a novel MRI molecular imaging probe, the relaxing mechanism of gadolinium fullerenes toward water molecules is different from the traditional gadolinium chelate. The embedded gadoliniumatoms or gadolinium clusters can indirectly relax water molecules through the outer carbon cage. The carbon cage has a large area of action, high efficiency and the dipole-dipole interaction between molecules, which further improves gadolinium fullerenes' relaxation efficiency. More than that, the embedded clusters could be protected through fullerenes. Because the carbon cages of fullerenes can prevent the attacking of metabolic products and leakage. Therefore, biological safety of gadolinium fullerenes is greatly improved [15]. However, the poor water solubility of metal fullerenes often limits its application in biomedicine. Therefore, research and preparation of water-soluble metal fullerene derivatives comes to be the primary problem that needs to be solved. The hollow carbon-cage structure of fullerenes can not only achieve good inclusion of gadolinium atoms, but also the surface structure of fullerenes can be easily modified a variety of water-soluble fullerenes. There were a few methods about surface modification, such as hydroxylated, carboxylated, PEGylated and so on [16]. A series of water-soluble lanthanide fullerenes as new magnetic resonance contrast agents were reported by Kato [17]. Compared with the water-insoluble Gd-DTPA, the relaxation ability of $Gd@C_{82}(OH)_n$ (n=30~40) has even reached 20 times of Gd-DTPA. Because Gd-based metallofullerenes had unique advantages, more and more new water-soluble gadolinium fullerene derivatives had been found, such as $Gd@C_{82}(OH)xOy$ [18,19], $Gd@C_{60}[C(COOH)_2]_{10}$ [20,21], $Gd_3N@C_{80}[DiPEG(OH)_x]_{13}$ [22] and so on. These water-soluble gadolinium fullerene derivatives exhibited great effect in biological imaging. Different gadolinium fullerenes derivatives exhibited varying relaxation rates. Compared to $Gd@C_{60,}$ $Gd@C_{82}$ was widely believed to possess superior relaxation properties due to its higher electron spin density and unique electronic structure. The hydroxyl functionalized gadofullerenes show significantly higher relaxivities than those of carboxylic derivatives [20,21].The hydroxylation modification of hemiketal structure $Gd@C_{82}(OH)xOy$ leaded to instability in its chemical structure, and the difference in the number of hydroxyl groups in the structure may result in diversity in relaxation rates [18].

To enhance the relaxation rates of gadolinium fullerenes, a novel MRI contrast agent water-soluble gadolinium fullerene nanoparticles $Gd@C_{82}$-TEG with clear

structure successfully were synthesized through a simple self assembly method. The chemical composition, particle size and morphology of these nanoparticles were analyzed and characterized by X-ray photoluminescence spectroscopy, laser nano-particle size instrument and transmission electron microscope. The Gd@C_{82} core coupled with the neutral and hydrophilic surface provided by TEG, exhibited high relaxivity, pronounced T_1-weighted MRI *in vitro* and no cytotoxicity.

Materials and methods

Materials

Gd@C_{82} fullerene was purchased from Xiamen Funano New Material Technology Co. Ltd. DMEM (dulbecco#39;s modified eagle medium) and Newborn Calf serum were purchased from Gibco. Human breast cancer cells were newly purchased from the Shanghai cell center.

Preparation of Gd@C_{82}-TEGs nanoparticles

The Gd@C_{82}-TEGs nanoparticles powders were obtained by the reaction of Gd@C_{82} fullerene solution [23–25] and tetraethylene glycol (TEG) under lithium hydroxide as catalyzer (Fig 1). The Gd@C_{82} fullerene solution (a solution of 1 mg/mL in 20 mL toluene), tetraethylene glycol (TEG, 20 mL) and lithium hydroxide(LiOH) (20 mg) were added into the reaction bottle in order. After reaction 20 hours, through adding excess ethyl acetate (EA), the obtained fullerene nanoparticles were precipitated. The obtained precipitate was dissolved in 20 mL of ultrapure water (18.2 MΩ·cm, 25°C), and the solution was loaded into a dialysis bag (molecular weight cutoff: 3.5 kDa). Dialysis was performed with ultrapure water for 48 h, resulting in a clear and transparent solution. The aqueous solution appeared darker. The post-dialysis solution was filtered through a 0.45 μm membrane filter. The filtrate was pre-frozen at −20 °C in a refrigerator, followed by lyophilization for 24 h to yield a brown powder. The powder was further dried for 48 h in a vacuum oven at 25 °C, then stored in a desiccator at ambient temperature.The weight of obtained Gd@C_{82}-TEGs nanoparticles powders was 30 mg.

Characterization of Gd@C_{82}-TEGs nanoparticles

At room temperature, 5 mg of Gd@C_{82}-TEGs nanoparticles was dissolved in redistilled water, ultrasonically dispersed homogeneously, and diluted. The particle size and distribution of the nanoparticles were measured using a laser nanoparticle size analyzer Nano-ZS90 at a wavelength of 633 nm.

The microscopic morphology of Gd@C_{82}-TEGs nanoparticles were measured through transmission electron microscopy (TEM) (JEOL-2100F) at 150 kV. Samples for TEM were prepared by directly dropping Gd@C_{82}-TEGs nanoparticles aqueous solution onto carbon-coated copper grids, dyeing with 2% phosphotungstic acid solution and drying at room temperature.

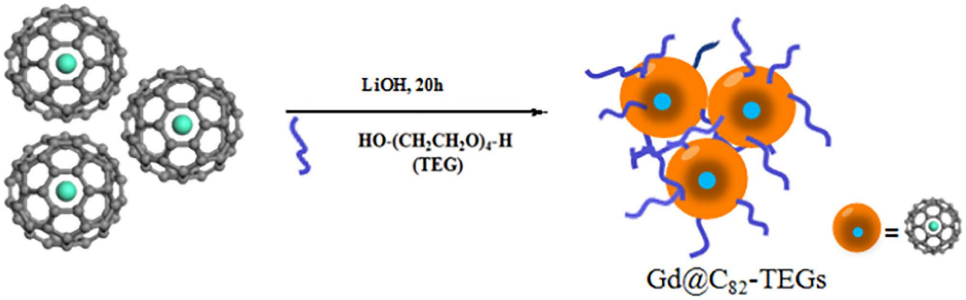

Fig 1. The preparation of Gd@C_{82}-TEGs nanoparticles.

https://doi.org/10.1371/journal.pone.0346592.g001

The chemical composition of Gd@C_{82}-TEGs nanoparticles were analyzed using X-ray photoluminescence spectroscopy (XPS). The X-ray photoelectron spectroscopy (XPS) was performed on Thermo K-Alpha, operating at 12 kV and 6 mA with an alumina target (Al kα, hv = 1486.68eV).The amount of Gd loaded on Gd@C_{82}-TEGs nanoparticles was determined by inductively coupled plasma-atomic emission spectrometry (ICP-AES, OPTIMA 5300DV).

The longitudinal (T_1) and transverse (T_2) relaxation times of the Gd@C_{82}-TEGs nanoparticles were determined by a 1.5 T clinical MR instrument (Sonata Siemens) at 37 °C by the T_1-weighted spin–echo method. The *in vitro* MRI phantomimages were acquired using a MicroMR-25 mini MR system (NiumagCorporation, Shanghai, China). The measurement parameters were as follows: T_1-weighted sequence, spin echo, TR/TE = 600/18.125 ms, matrix acquisition = 128 × 128, NS = 2, FOV = 100 mm × 100 mm, Slice Thickness/Gap = 3 mm/0.5 mm, 0.50 T, 32.0 °C. The values of T_1 and T_2 were determined by inversion-recovery and Carr-Pucell-Meiboom-Gill method respectively. Through the fitting of the $1/T_1$ and Gd^{3+}concentration, the r_1 value was obtained. Consistent with the above method, the r_2 value was obtained by fitting between $1/T_2$ and Gd^{3+}concentration.

In vitro cytotoxicity of the Gd@C_{82}-TEGs nanoparticles

A standard MTT (3-(4,5-dimethylthiazolyl-2)-2,5-diphenyl tetrazolium bromide) assay was conducted using a human breast cancer cell line (MCF-7) to estimate the *in vitro* cytotoxicity of Gd@C_{82}-TEGs nanoparticles. The preparation of MCF-7 cells and disinfection of Gd@C_{82}-TEGs nanoparticles were referred to the previous work [26].

Inoculate prpared MCF-7 cells into a 96 well plate with a cell density of 6 × 10^5 cells per well, and incubate in a moist atmosphere with 5% CO_2 in 37 °C culture medium for 24 hours. Then take out the culture medium and mix the cells with those containing 100 μL Gd@C_{82}-TEGs nanoparticles with different concentrations (0, 25, 50, and 100 mg/L). The mixture were continued to incubate at the above same condition for 48 hours.

The cell viabilities of Gd@C_{82}-TEGs nanoparticles against MCF-7 cells were assessed using MTT. The concrete method was referred to reference [8].

Results and discussion

Characterization of Gd@C_{82}-TEGs nanoparticles

The water-soluble Gd@C_{82}-TEGs nanoparticles as a novel MRI contrast agent were synthesized via the metal fullerenes Gd@C_{82} assembled with tetraethylene glycol (TEG) for 20 h (Fig 1). Lithium hydroxide acts as a base catalyst that promotes cage-opening of C_{82} via nucleophilic attack, facilitating the incorporation of oxygen into the π-conjugated framework to form oxygen-functionalized derivatives.

The particle size and distribution of Gd@C_{82}-TEGs nanoparticles were determined by dynamic light scattering (DLS). Fig 2 showed the particle size distribution of Gd@C_{82}-TEGs nanoparticles. The average particle size of Gd@C_{82}-TEGs nanoparticles was 97 nm. The size of nanoparticles directly affects their longitudinal relaxivity and *in vivo* clearance pathways. It is well known that nanoparticles <5 nm are rapidly cleared by renal filtration, limiting imaging duration, whereas those >100 nm are sequestered by liver and spleen macrophages, impairing target accumulation. The average particle size of Gd@C_{82}-TEGs nanoparticles could effectively evade rapid clearance by the reticuloendothelial system, prolong circulation time, enhance accumulation in tumor tissues via the enhanced permeability and retention effect, and thereby achieve high relaxivity and prolonged circulation.

The morphology of the nanoparticles was observed by TEM in Fig 3. The nanoparticles with spherical distribution were observed and had good dispersibility and no aggregation. The spherical configuration ensured complete encapsulation of Gd^3 within the C_{82} carbon cage, preventing the leakage of free gadolinium and reducing the risk of nephrogenic systemic fibrosis. [27] From the enlarged electron micrograph, it can be seen that small black metal clusters are gathered inside the carbon cage structure of fullerene. The average size of nanoparticles was about 100 nm, which was consistent with the analysis of DLS.

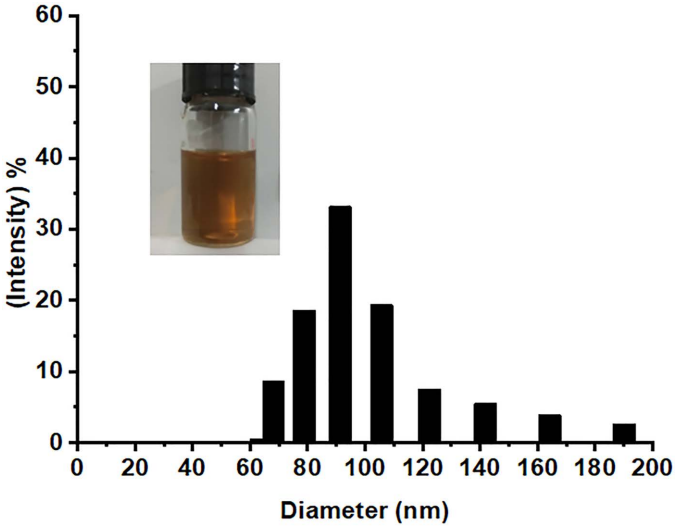

Fig 2. The particle size of Gd@C_{82}-TEGs nanoparticles.

https://doi.org/10.1371/journal.pone.0346592.g002

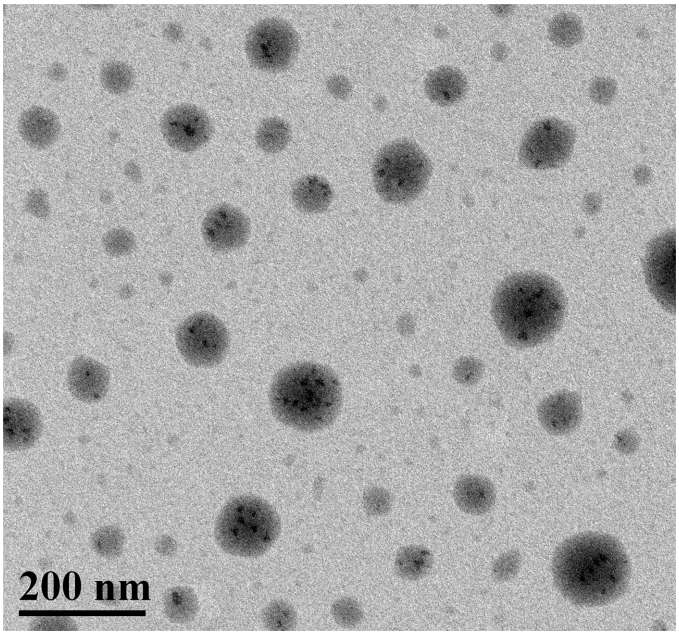

Fig 3. The TEM image of the Gd@C_{82}-TEGs nanoparticles.

https://doi.org/10.1371/journal.pone.0346592.g003

The C ^{1}S XPS spectrum of Gd@C_{82}-TEGs nanoparticles exhibited three well-resolved peaks at binding energies of 284.8 eV, 286.3 eV, and 289.0 eV, which were assigned to C=C–C, C–O, and C=O species, respectively (Fig 4). These XPS data uniformly indicated that the conjugated framework of the pristine C_{82} fullerene was opened and covalently bonded to the triethylene glycol (TEG) moiety through a nucleophilic addition pathway, resulting in a C_{82}–O–R linkage,

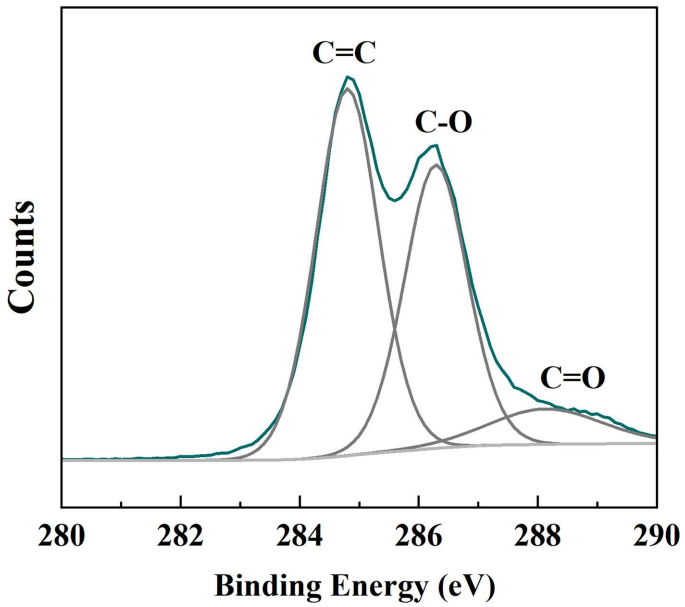

Fig 4. The C ^{1}S XPS spectrum of the Gd@C_{82}-TEGs nanoparticles.

https://doi.org/10.1371/journal.pone.0346592.g004

despite the coexistence of a considerable amount of ketone (C=O) functionality. After calculated according to ICP-AES, the loading Gd amount in Gd@C_{82}-TEGs nanoparticles was 8.0 wt%.

In vitro MRI performance

To verify whether Gd@C_{82}-TEGs nanoparticles possess effective T_1-weighted, the proton relaxivity (r_1) and transverse relaxivity (r_2) with different Gd^{3+} concentration were determined. The concrete data were seen in Fig 5.

It could be seen that the r_1 value of the Gd@C_{82}-TEGs nanoparticles was high up to 37.1 $mM^{-1}{\cdot}s^{-1}$ in Fig 5A. The r_1 value was far higher than that of the commercial Magnevist (Gd-DTPA, 3.19 $mM^{-1}{\cdot}s^{-1}$). The appealing MRI enhancement ability of the Gd@C_{82}-TEGs nanoparticles may attribute to the large area of the outer carbon cage, through which the embedded gadolinium atoms can efficiently and indirectly relax the water molecules. Moreover, the dipole-dipole interaction between the molecules further improved its relaxation efficiency. Notably, the transverse relaxivity (r_2) was 64.9 $mM^{-1}{\cdot}s^{-1}$ (Fig 5B), which greater than that of commercial Magnevist under the same conditions. Usually, the r_2/r_1 ratios of T_1 agents were 1-2, while that of T_2 agents is up to 10 or more. The r_2/r_1 ratio ($r_2/r_1 = 1.74 < 2$) at 0.50 T magnetic fields of Gd@C_{82}-TEGs nanoparticles maybe beneficial for T_1-weighted contrast effect.

T_1-weighted MRI of Gd@C_{82}-TEGs nanoparticles at varying Gd^{3+} concentrations ranging from 0 to 1.5 mM and Gd-DTPA(1.0 mM) in H_2O were shown in Fig 6. Under the same Gd^{3+} concentration, the MRI signal-enhancing efficiency of Gd@C_{82}-TEGs nanoparticles was superior to that of Gd-DTPA. The results were in agreement with the proton relaxivity analysis.

In vitro cytotoxicity of the Gd@C_{82}-TEGs nanoparticles

The *in vitro* cytotoxicity of the Gd@C_{82}-TEGs nanoparticles against human breast cancer MCF-7 cells was assayed by MTT. It could be observed that there was no cell toxicity through 24 h and 48 h incubation in Fig 7. The relative viability remained above 80% in the concentration range of 12.5–100 mg/L. Even after incubation for 48 hours at a concentration of 100 mg/L, it remained as high as 82%.

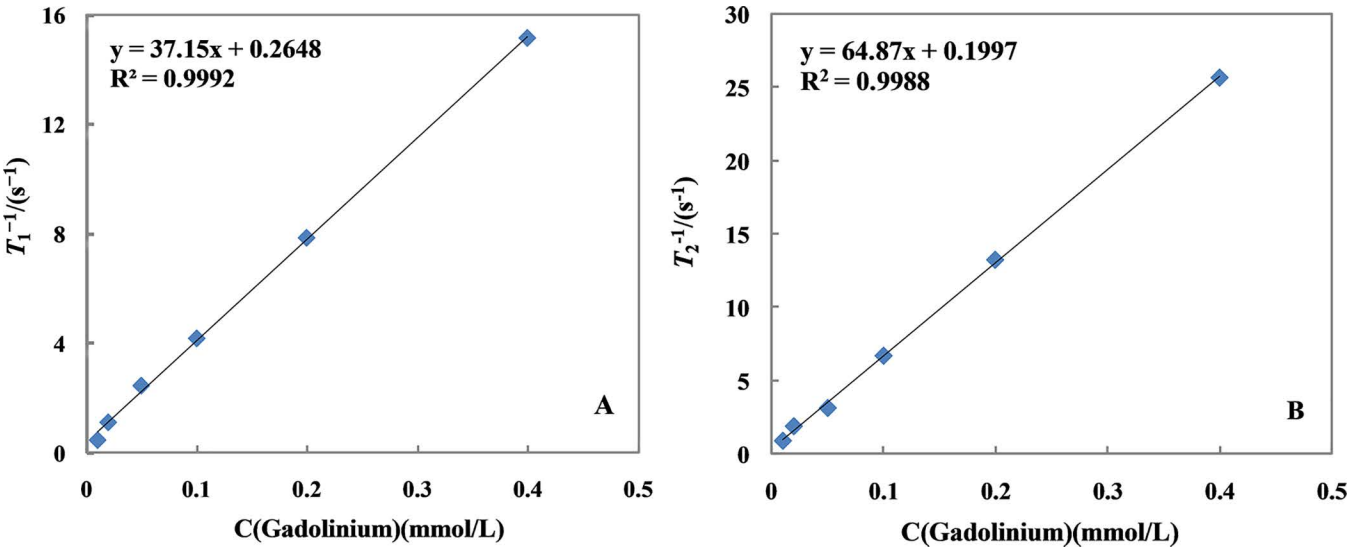

Fig 5. Plots of $1/T_1$ (A) or $1/T_2$ (B) *versus* Gd^{3+} concentration.

https://doi.org/10.1371/journal.pone.0346592.g005

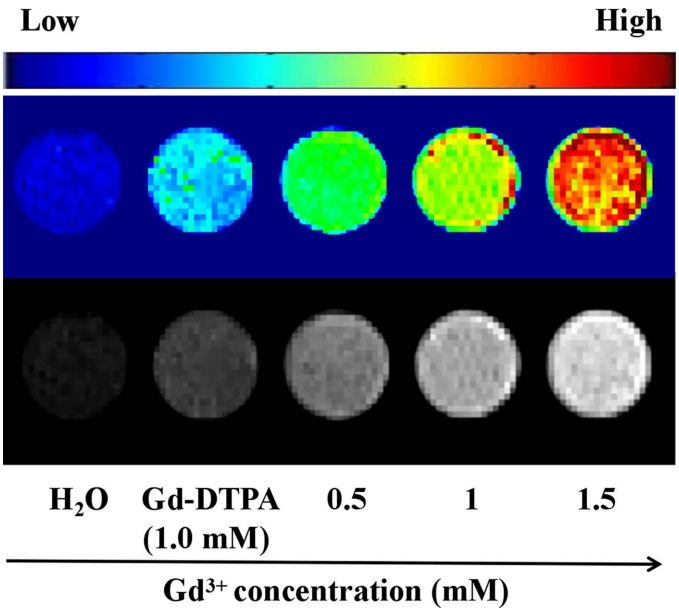

Fig 6. T_1-weighted MRI of Gd@C_{82}-TEGs nanoparticles at varied [Gd^{3+}] (0 - 1.5 mM) and Gd-DTPA(1.0 mM) in H_2O.

https://doi.org/10.1371/journal.pone.0346592.g006

The morphology of MCF-7 cells was observed by a microscope. As shown in Fig 8, the morphology and structure of each group MCF-7 cells did not change after incubated with different concentrations (0, 25, 50, and 100 mg/L) of Gd@C_{82}-TEGs nanoparticles for 48 h, and the morphology of MCF-7 cells in each group remained well. This indirectly indicated that the fullerene carbon cage could encapsulate the gadolinium atoms well, and the preparation method of Gd@C_{82}-TEGs nanoparticles cannot change the structure of the fullerene so that the Gd@C_{82}-TEGs nanoparticles will not produce obvious toxicity to cells.

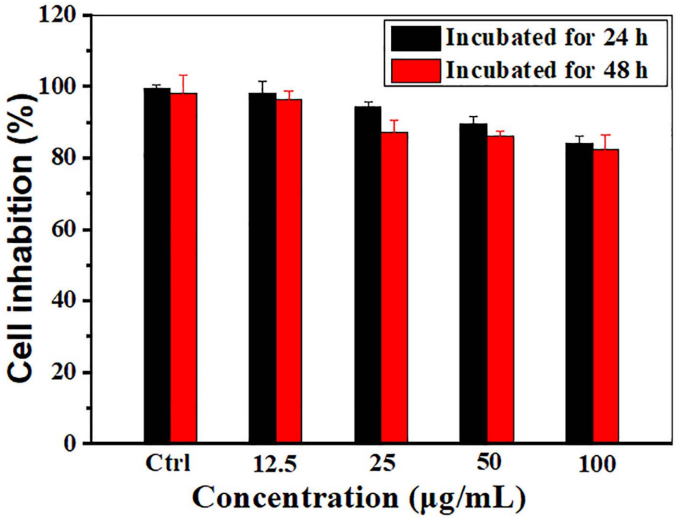

Fig 7. Cytotoxicity of the Gd@C_{82}-TEGs nanoparticles in MCF-7 cells after 24 and 48 h incubation.

https://doi.org/10.1371/journal.pone.0346592.g007

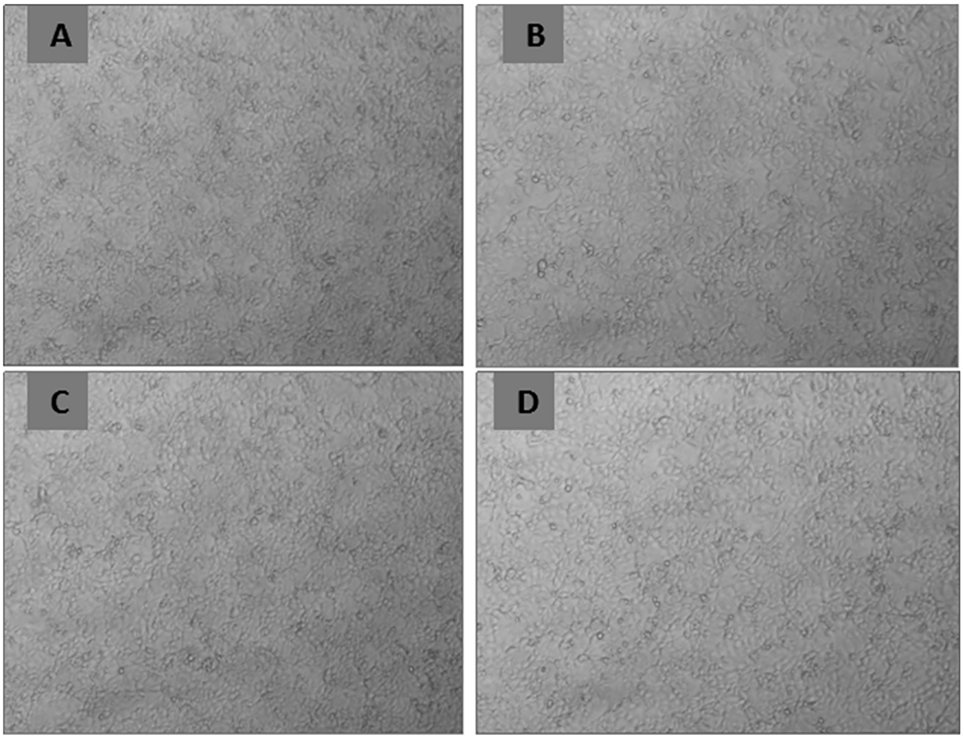

Fig 8. Morphology of MCF-7 cells with Gd@C_{82}-TEGs nanoparticles (0- 100 μg/mL).

https://doi.org/10.1371/journal.pone.0346592.g008

Conclusion

The water-soluble Gd@C_{82}-TEGs nanoparticles as a novel MRI contrast agent were synthesized by a simple, effective and environmentally friendly self assembly method. The 97 nm spherical shape of Gd@C_{82}-TEG nanoparticles ensured

high relaxivity. The proton relaxivity (r_1) and transverse relaxivity (r_2) were high up to 37.1 $mM^{-1}{\cdot}s^{-1}$ and 64.9 $mM^{-1}{\cdot}s^{-1}$, which greater than that of commercial Magnevist under the same conditions. The obtained Gd@C_{82}-TEGs nanoparticles showed noticeable T_1-weighted MRI *in vitro*. Besides, the *in vitro* cytotoxicity experiments confirmed that the Gd@C_{82}-TEGs nanoparticles had no significant effect on cell metabolism and structure, and the survival rate of cells was more than 82% after incubation for 48 hours at a concentration of 100 mg/L, which indicated that the as-prepared Gd@C_{82}-TEGs nanoparticles were no cytotoxicity. The Gd@C_{82}-TEGs nanoparticles are expected to serve as efficient MRI contrast agents for biomedical imaging.

Author contributions

Conceptualization: Wanyun Liu.

Data curation: Ping Huo, Xiuming Zhou, Dayan Xiong.

Formal analysis: Dayan Xiong.

Funding acquisition: Wanyun Liu.

Investigation: Ping Huo, Xiuming Zhou, Dayan Xiong.

Resources: Xiuming Zhou.

Writing – original draft: Xiuming Zhou, Dayan Xiong.

Writing – review & editing: Ping Huo.

References

1. Mansfield P. Snapshot magnetic resonance imaging (Nobel lecture). Angew Chem Int Ed Engl. 2004;43(41):5456–64. https://doi.org/10.1002/anie.200460078 PMID: 15384128
2. Feng Y, Murphy MC, Hojo E, Li F, Roberts N. Magnetic Resonance Elastography in the Study of Neurodegenerative Diseases. J Magn Reson Imaging. 2024;59(1):82–96. https://doi.org/10.1002/jmri.28747 PMID: 37084171
3. Ma Q, Luo Y, Li Y, Xu S, Wang L. Ultrasmall hydrophilic Gd-free contrast agents via ligand directed hydrolysis for efficient magnetic resonance imaging. Adv Funct Mater. 2025;35(28):1. https://doi.org/10.1002/adfm.202422876
4. Eisen A, Fletcher GG, Fienberg S, George R, Holloway C, Kulkarni S, et al. Breast Magnetic Resonance Imaging for Preoperative Evaluation of Breast Cancer: A Systematic Review and Meta-Analysis. Can Assoc Radiol J. 2024;75(1):118–35. https://doi.org/10.1177/08465371231184769 PMID: 37593787
5. Schwarz L, Unger E, Gahleitner A, Rausch-Fan X, Jonke E. A novel approach for gingiva thickness measurements around lower anterior teeth by means of dental magnetic resonance imaging. Clin Oral Investig. 2023;28(1):18. https://doi.org/10.1007/s00784-023-05459-4 PMID: 38135801
6. Xiao Y, Wu Y-J, Zhang W-J, Li X-J, Pei F-K. Research Progress of Magnetic Resonance Imaging Contrast Agents. Chinese Journal of Analytical Chemistry. 2011;39(5):757–64. https://doi.org/10.1016/s1872-2040(10)60438-0
7. Fatouros PP, Corwin FD, Chen Z-J, Broaddus WC, Tatum JL, Kettenmann B, et al. In vitro and in vivo imaging studies of a new endohedral metallofullerene nanoparticle. Radiology. 2006;240(3):756–64. https://doi.org/10.1148/radiol.2403051341 PMID: 16837672
8. Caravan P, Ellison JJ, McMurry TJ, Lauffer RB. Gadolinium(III) Chelates as MRI Contrast Agents: Structure, Dynamics, and Applications. Chem Rev. 1999;99(9):2293–352. https://doi.org/10.1021/cr980440x PMID: 11749483
9. Yang L, Beija M, Laurent S, Elst LV, Muller RN, Duong HTT, et al. Macromolecular ligands for gadolinium MRI contrast agents. Macromolecules. 2012;45:4196–204. https://doi.org/10.1021/ma300521c
10. Franano FN, Edwards WB, Welch MJ, Brechbiel MW, Gansow OA, Duncan JR. Biodistribution and metabolism of targeted and nontargeted protein-chelate-gadolinium complexes: evidence for gadolinium dissociation in vitro and in vivo. Magn Reson Imaging. 1995;13(2):201–14. https://doi.org/10.1016/0730-725x(94)00100-h PMID: 7739361
11. Wedeking P, Kumar K, Tweedle MF. Dissociation of gadolinium chelates in mice: relationship to chemical characteristics. Magn Reson Imaging. 1992;10(4):641–8. https://doi.org/10.1016/0730-725x(92)90016-s PMID: 1501535
12. Bahl M. The Quest to Reduce the Use of Gadolinium-based Contrast Agents: AI May Provide a Solution. Radiology. 2023;307(3):e230325. https://doi.org/10.1148/radiol.230325 PMID: 36943082
13. Lenkinski RE, Rofsky NM. Contrast Media-driven Anthropogenic Gadolinium: Knowns and Unknowns. Radiology. 2024;311(1):e240020. https://doi.org/10.1148/radiol.240020 PMID: 38652027

14. Li J, Yang W, Cui R, Wang D, Chang Y, Gu W, et al. Metabolizer in vivo of fullerenes and metallofullerenes by positron emission tomography. Nanotechnology. 2016;27(15):155101. https://doi.org/10.1088/0957-4484/27/15/155101 PMID: 26926042
15. Tagmatarchis N, Shinohara H. Fullerenes in medicinal chemistry and their biological applications. Mini Rev Med Chem. 2001;1(4):339–48. https://doi.org/10.2174/1389557013406684 PMID: 12369961
16. Li T, Dorn HC. Biomedical Applications of Metal-Encapsulated Fullerene Nanoparticles. Small. 2016;13(8). https://doi.org/10.1002/smll.201603152
17. Kato H, Kanazawa Y, Okumura M, Taninaka A, Yokawa T, Shinohara H. Lanthanoid endohedral metallofullerenols for MRI contrast agents. J Am Chem Soc. 2003;125(14):4391–7. https://doi.org/10.1021/ja027555+ PMID: 12670265
18. Zou T, Zhen M, Li J, Chen D, Feng Y, Li R, et al. The effect of hemiketals on the relaxivity of endohedral gadofullerenols. RSC Adv. 2015;5(117):96253–7. https://doi.org/10.1039/c5ra16620a
19. Xing G, Yuan H, He R, Gao X, Jing L, Zhao F, et al. The strong MRI relaxivity of paramagnetic nanoparticles. J Phys Chem B. 2008;112(20):6288–91. https://doi.org/10.1021/jp8012706 PMID: 18433163
20. Bolskar RD, Benedetto AF, Husebo LO, Price RE, Jackson EF, Wallace S, et al. First soluble M@C60 derivatives provide enhanced access to metallofullerenes and permit in vivo evaluation of Gd@C60[C(COOH)2]10 as a MRI contrast agent. J Am Chem Soc. 2003;125(18):5471–8. https://doi.org/10.1021/ja0340984 PMID: 12720461
21. Tóth E, Bolskar RD, Borel A, González G, Helm L, Merbach AE, et al. Water-soluble gadofullerenes: toward high-relaxivity, pH-responsive MRI contrast agents. J Am Chem Soc. 2005;127(2):799–805. https://doi.org/10.1021/ja044688h PMID: 15643906
22. Zhang J, Fatouros PP, Shu C, Reid J, Owens LS, Cai T, et al. High relaxivity trimetallic nitride (Gd3N) metallofullerene MRI contrast agents with optimized functionality. Bioconjug Chem. 2010;21(4):610–5. https://doi.org/10.1021/bc900375n PMID: 20218678
23. Jeong J, Jung J, Choi M, Kim JW, Chung SJ, Lim S, et al. Color-tunable photoluminescent fullerene nanoparticles. Adv Mater. 2012;24(15):1999–2003. https://doi.org/10.1002/adma.201104772 PMID: 22431377
24. Liu W, Wei J, Chen Y. Electrospun poly(l-lactide) nanofibers loaded with paclitaxel and water-soluble fullerenes for drug delivery and bioimaging. New J Chem. 2014;38(12):6223–9. https://doi.org/10.1039/c4nj01259c
25. Liu W, Wei J, Chen Y, Huo P, Wei Y. Electrospinning of poly(L-lactide) nanofibers encapsulated with water-soluble fullerenes for bioimaging application. ACS Appl Mater Interfaces. 2013;5(3):680–5. https://doi.org/10.1021/am400037s PMID: 23327807
26. Liu W, Wei J, Huo P, Lu Y, Chen Y, Wei Y. Controlled release of brefeldin A from electrospun PEG-PLLA nanofibers and their in vitro antitumor activity against HepG2 cells. Mater Sci Eng C Mater Biol Appl. 2013;33(5):2513–8. https://doi.org/10.1016/j.msec.2013.02.013 PMID: 23623062
27. Zhang KK, Wang C, Zhang MH, Bai ZB, Xie FF, Tan YZ, et al. A Gd@C82 single-molecule electret. Nature Nanotechnology. 2020;15:1019–24. https://doi.org/10.1038/s41565-020-00778-z